

# UC San Diego

## UC San Diego Previously Published Works

### Title

SARS-CoV-2 Omicron (B.1.1.529) shows minimal neurotropism in a double-humanized mouse model

### Permalink

<https://escholarship.org/uc/item/4jp6x89n>

### Authors

Alves, Rubens Prince Dos Santos

Wang, Ying-Ting

Mikulski, Zbigniew

et al.

### Publication Date

2023-04-01

### DOI

10.1016/j.antiviral.2023.105580

### Copyright Information

This work is made available under the terms of a Creative Commons Attribution-NonCommercial-NoDerivatives License, available at

<https://creativecommons.org/licenses/by-nc-nd/4.0/>

Peer reviewed



Since January 2020 Elsevier has created a COVID-19 resource centre with free information in English and Mandarin on the novel coronavirus COVID-19. The COVID-19 resource centre is hosted on Elsevier Connect, the company's public news and information website.

Elsevier hereby grants permission to make all its COVID-19-related research that is available on the COVID-19 resource centre - including this research content - immediately available in PubMed Central and other publicly funded repositories, such as the WHO COVID database with rights for unrestricted research re-use and analyses in any form or by any means with acknowledgement of the original source. These permissions are granted for free by Elsevier for as long as the COVID-19 resource centre remains active.



## SARS-CoV-2 Omicron (B.1.1.529) shows minimal neurotropism in a double-humanized mouse model

Rubens Prince dos Santos Alves<sup>a,1</sup>, Ying-Ting Wang<sup>a,1</sup>, Zbigniew Mikulski<sup>c</sup>, Sara McArdle<sup>c</sup>, Norazizah Shafee<sup>a</sup>, Kristen M. Valentine<sup>a</sup>, Robyn Miller<sup>a</sup>, Shailendra Kumar Verma<sup>a</sup>, Fernanda Ana Sosa Batiz<sup>a</sup>, Erin Maule<sup>a</sup>, Michael N. Nguyen<sup>a</sup>, Julia Timis<sup>a</sup>, Colin Mann<sup>a</sup>, Michelle Zandonatti<sup>a</sup>, Suzie Alarcon<sup>d</sup>, Jenny Rowe<sup>e</sup>, Mitchell Kronenberg<sup>f</sup>, Daniela Weiskopf<sup>a</sup>, Alessandro Sette<sup>a,8</sup>, Kathryn Hastie<sup>a</sup>, Erica Ollmann Saphire<sup>a</sup>, Stephen Festin<sup>e</sup>, Kenneth Kim<sup>b,\*,\*,1</sup>, Sujan Shresta<sup>a,\*</sup>

<sup>a</sup> Center for Infectious Disease and Vaccine Research, La Jolla Institute for Immunology, La Jolla, CA, USA

<sup>b</sup> Histopathology Core Facility, La Jolla Institute for Immunology, La Jolla, CA, USA

<sup>c</sup> Microscopy and Histology Core Facility, La Jolla Institute for Immunology, La Jolla, CA, USA

<sup>d</sup> Sequencing Core Facility, La Jolla Institute for Immunology, La Jolla, CA, USA

<sup>e</sup> Charles River Laboratories Research Models and Services Inc., Wilmington, MA, USA

<sup>f</sup> Division of Developmental Immunology, La Jolla Institute for Immunology, La Jolla, CA, USA

<sup>8</sup> Department of Medicine, Division of Infectious Diseases and Global Public Health, University of California, San Diego, La Jolla, CA, 92037, USA

### ARTICLE INFO

#### Keywords:

SARS-CoV-2  
 COVID-19  
 Omicron  
 Brain  
 Neurotropism  
 Mouse model  
 Human ACE2  
 Human CD34 immune cells  
 T cell  
 NCG

### ABSTRACT

Although severe acute respiratory syndrome coronavirus-2 (SARS-CoV-2) initially infects the respiratory tract, it also directly or indirectly affects other organs, including the brain. However, little is known about the relative neurotropism of SARS-CoV-2 variants of concern (VOCs), including Omicron (B.1.1.529), which emerged in November 2021 and has remained the dominant pathogenic lineage since then. To address this gap, we examined the relative ability of Omicron, Beta (B.1.351), and Delta (B.1.617.2) to infect the brain in the context of a functional human immune system by using human angiotensin-converting enzyme 2 (hACE2) knock-in triple-immunodeficient NCG mice with or without reconstitution with human CD34<sup>+</sup> stem cells. Intranasal inoculation of huCD34<sup>+</sup>-hACE2-NCG mice with Beta and Delta resulted in productive infection of the nasal cavity, lungs, and brain on day 3 post-infection, but Omicron was surprisingly unique in its failure to infect either the nasal tissue or brain. Moreover, the same infection pattern was observed in hACE2-NCG mice, indicating that antiviral immunity was not responsible for the lack of Omicron neurotropism. In independent experiments, we demonstrate that nasal inoculation with Beta or with D614G, an ancestral SARS-CoV-2 with undetectable replication in huCD34<sup>+</sup>-hACE2-NCG mice, resulted in a robust response by human innate immune cells, T cells, and B cells, confirming that exposure to SARS-CoV-2, even without detectable infection, is sufficient to induce an antiviral immune response. Collectively, these results suggest that modeling of the neurologic and immunologic sequelae of SARS-CoV-2 infection requires careful selection of the appropriate SARS-CoV-2 strain in the context of a specific mouse model.

### 1. Introduction

Severe respiratory syndrome coronavirus-2 (SARS-CoV-2) is an enveloped, positive-sense, single-stranded RNA virus, and it is the

etiologic agent of the COVID-19 pandemic (Zhu et al., 2020). Between May and November 2020, four major SARS-CoV-2 variants of concern (VOCs) emerged in rapid succession; Alpha (B.1.1.7), Beta (B.1.351), Gamma (P.1.), and Delta (B.1.617.2) (Li et al., 2022), but the next major

\* Corresponding author.

\*\* Corresponding author.

E-mail addresses: [kenneth@lji.org](mailto:kenneth@lji.org) (K. Kim), [sujan@lji.org](mailto:sujan@lji.org) (S. Shresta).

<sup>1</sup> These authors contributed equally.

VOC, Omicron (B.1.1.529), was not detected until November 2021 and no additional VOCs have emerged since then. Thus, considerable attention has been paid to understanding Omicron sublineage evolution and its impact on escape of vaccine-induced and convalescent immunity and on the acute and long-term pathologic sequelae of COVID-19 (Starr et al., 2022; Focosi et al., 2022; Cao et al., 2022).

Although SARS-CoV-2 initially infects the upper respiratory tract, accumulating evidence indicates that it has direct or indirect effects on other organs, including the brain. Neurological manifestations include headache and brain fog (Dangayach et al., 2022). An increased risk for new diagnosis of Alzheimer's disease within one year of infection has also been noted (Wang et al., 2022). Notably, a recent retrospective study suggested that the risk of cognitive deficit, dementia, psychotic disorder, and epilepsy or seizures remains elevated for 2 years after SARS-CoV-2 infection (Taquet et al., 2022). Moreover, the risk profiles of individual neurological and psychiatric manifestations were similar just before vs just after the emergence of Alpha but were increased to a similar extent just after vs just before the emergence of Delta and Omicron, suggesting that there may be strain-specific mechanistic differences underlying brain-related pathologies. The brain may be indirectly affected via mechanisms such as inflammation (Perry et al., 2007), viral protein migration (Rhea et al., 2021), and altered blood and cerebrospinal fluid circulation (Crunfli et al., 2022); but there is also evidence of direct infection from multiple autopsy studies demonstrating the presence of viral RNA and antigen in the brain (Serrano et al., 2022; Satrwar et al., 2021; ea, 2021).

Animal models that recapitulate the phenotypes observed in SARS-CoV-2-infected humans are an essential tool for understanding pathogenesis. Several studies using non-human primate, wild-type mouse, and transgenic mouse models have also demonstrated the presence of SARS-CoV-2 RNA, antigen, and infectious virus in the brain (Rutkai et al., 2022; Bishop et al., 2022; Vidal et al., 2021; de Oliveira et al., 2022; Zhang et al., 2021; Fernández-Castañeda et al., 2022; Shang et al., 2022) and suggest that direct and indirect routes may contribute to brain-related pathologies. Most non-adapted SARS-CoV-2 strains replicate poorly in standard wild-type mouse strains due to sequence differences between human and mouse angiotensin-converting enzyme 2 (ACE2), the major SARS-CoV-2 receptor. The most commonly used mouse model to date is the K18-hACE2 mouse, in which hACE2 expression is driven by the epithelial cell cytokeratin-18 gene promoter (McCray et al., 2007). Intranasal inoculation of these mice has been shown to result in cerebral infection and death, possibly due to the presence of multiple copies of hACE2 transgene (Kumari et al., 2021; Winkler et al., 2022). However, brain infection is reduced in K18-hACE2 mice following SARS-CoV-2 inoculation via aerosol exposure (Fumagalli et al., 2022), which is likely most similar to the route of human exposure. Moreover, there is evidence for SARS-CoV-2 VOC-specific differences in neurotropism; for example, nasal infection of immunocompetent hamsters indicate that Omicron has no neurotropism or reduced neurotropism compared to SARS-CoV-2 D614G (Bauer et al., 2022; Mohandas et al., 2022; Armando et al., 2022), and recent studies suggest that VOCs exhibit differing degrees of neurotropism also in K18-hACE2 mice (Chan et al., 2022; Seehusen et al., 2022; Natekar et al., 2022). These findings suggest that not only the animal model but also the specific SARS-CoV-2 VOC influence invasion and infection of the brain, and thus affect the utility of the model for studies of the neurologic sequelae of COVID-19.

One advantage to the use of mice for modeling of SARS-CoV-2 infection and COVID-19 is the availability of immunodeficient, human immune-reconstituted, and transgenic strains, making it possible to assess the importance of both viral and host factors in infection and disease development (Kenney et al., 2022; Fu et al., 2021; Shang et al., 2021; Wahl et al., 2021; Sefik et al., 2021, 2022; Mao et al., 2021). In the present study, we employed human ACE2 knock-in (NOD/ShiLtJGpt-Prkdc<sup>em26Cd52</sup>IL2rg<sup>em26Cd22</sup>Ace2<sup>em1Cin(hACE2)</sup>/GptCRL) or mouse ACE2 (NOD-Prkdc<sup>em26Cd52</sup>IL2rg<sup>em26Cd22</sup>/NjuCrl) triple-immuno

deficient (NCG) mice, which lack functional mouse T-, B-, and natural killer (NK) cells, and have reduced numbers of dendritic cells and macrophages (Eberle et al., 2020; Tarpinian et al., 2020). Myeloablation of NCG mice followed by reconstitution with human umbilical cord blood-derived CD34<sup>+</sup> stem cells generates double-humanized huCD34<sup>+</sup>-hACE2-NCG or huCD34<sup>+</sup>-mACE2-NCG mice, which have a broad range of circulating and tissue-associated human immune cells (Shultz et al., 2007). Previous studies with NCG mice have demonstrated that human immune cells take residence in mouse tissues, including the lungs, for months after stem cell engraftment (Eberle et al., 2020). Importantly, apheresis prior to engraftment ensures that no anti-SARS-CoV-2 antibodies present in cord blood are passively transferred with the graft.

In the present study, we compared the ability of SARS-CoV-2 Omicron, Beta, and Delta to replicate in the nasal cavities, lungs, and brain of NCG mice expressing mouse ACE2 or hACE2 with or without huCD34<sup>+</sup> cell engraftment; to inflict lung damage in huCD34<sup>+</sup>-hACE2-NCG mice; and, in independent experiments, to determine the ability of SARS-CoV-2 strains with detectable vs undetectable replication in huCD34<sup>+</sup>-mACE2-NCG mice to elicit functional human innate and adaptive immune responses. Notably, we found that Omicron failed to exhibit neurotropism in both human immune-reconstituted and immunodeficient mice. Because neurologic sequelae are seen in clinical Omicron infection and this lineage has not yet been recovered from the human brain (Zhang et al., 2023), Omicron may thus serve as an important lineage for studies of SARS-CoV-2's indirect causes of neurocognitive dysfunction. We additionally show that SARS-CoV-2 exposure, without detectable infection of the respiratory tract, is sufficient to induce a robust human immune response in these mice.

## 2. Results

### 2.1. SARS-CoV-2 Beta (B.1.351), Delta (B.1.617.2), and Omicron (B.1.1.529 BA.2) show distinct capacities to replicate in the upper and lower respiratory tracts of huCD34<sup>+</sup>-hACE2-NCG mice

To begin to evaluate huCD34<sup>+</sup>-hACE2-NCG mice as a SARS-CoV-2 model, we intranasally (i.n.) inoculated mice with 10<sup>4</sup> plaque-forming units (PFU) of SARS-CoV-2 Beta, Delta, or Omicron BA.2. The Beta and Delta VOC were etiologies for their respective waves of the COVID-19 pandemic in the spring and latter half of 2021 (WHO, 2023), whereas in the spring of 2022 Omicron sublineage BA.2 accounted for up to 90% of SARS-CoV-2 cases in this part of the Omicron wave (Elliott et al., 2022). We measured viral 7a subgenomic RNA (sgRNA) levels by qRT-PCR in nasal turbinates and lungs at 3 days post-infection (p.i.). We detected similar levels of Beta and Delta sgRNA in both nasal turbinates and lungs, but strikingly, sgRNA was not detectable in the nasal turbinates of Omicron-infected mice, and sgRNA levels in the lungs were significantly reduced (Fig. 1A, left). Consistent with the sgRNA data, higher levels of infectious Beta and Delta, as measured by plaque assay on Vero E6 cells, were present in the lung than Omicron at day 3 p.i. (Fig. 1A, right). To evaluate the sites of SARS-CoV-2 pulmonary infection, we performed immunofluorescence (IF) staining of SARS-CoV-2 nucleocapsid (N) protein in the lungs of mice infected with Beta, Delta, or Omicron. At day 3 p.i. the N protein of each VOC was localized primarily to the cytoplasm of bronchiolar epithelial cells (BECs; Fig. 1B), but it was also present in the cytoplasm of occasional cells in the alveolar interstitium (data not shown). Thus, while huCD34<sup>+</sup>-hACE2-NCG mice permit productive infection of lung BECs by Beta, Delta, and Omicron variants, Omicron is uniquely unable to infect the nasal cavity and exhibits reduced tropism to the lungs.

### 2.2. SARS-CoV-2 Beta, Delta, and Omicron induce similar levels and types of bronchiole injury in huCD34<sup>+</sup>-hACE2-NCG mice

Because the pattern of respiratory tract infection differed

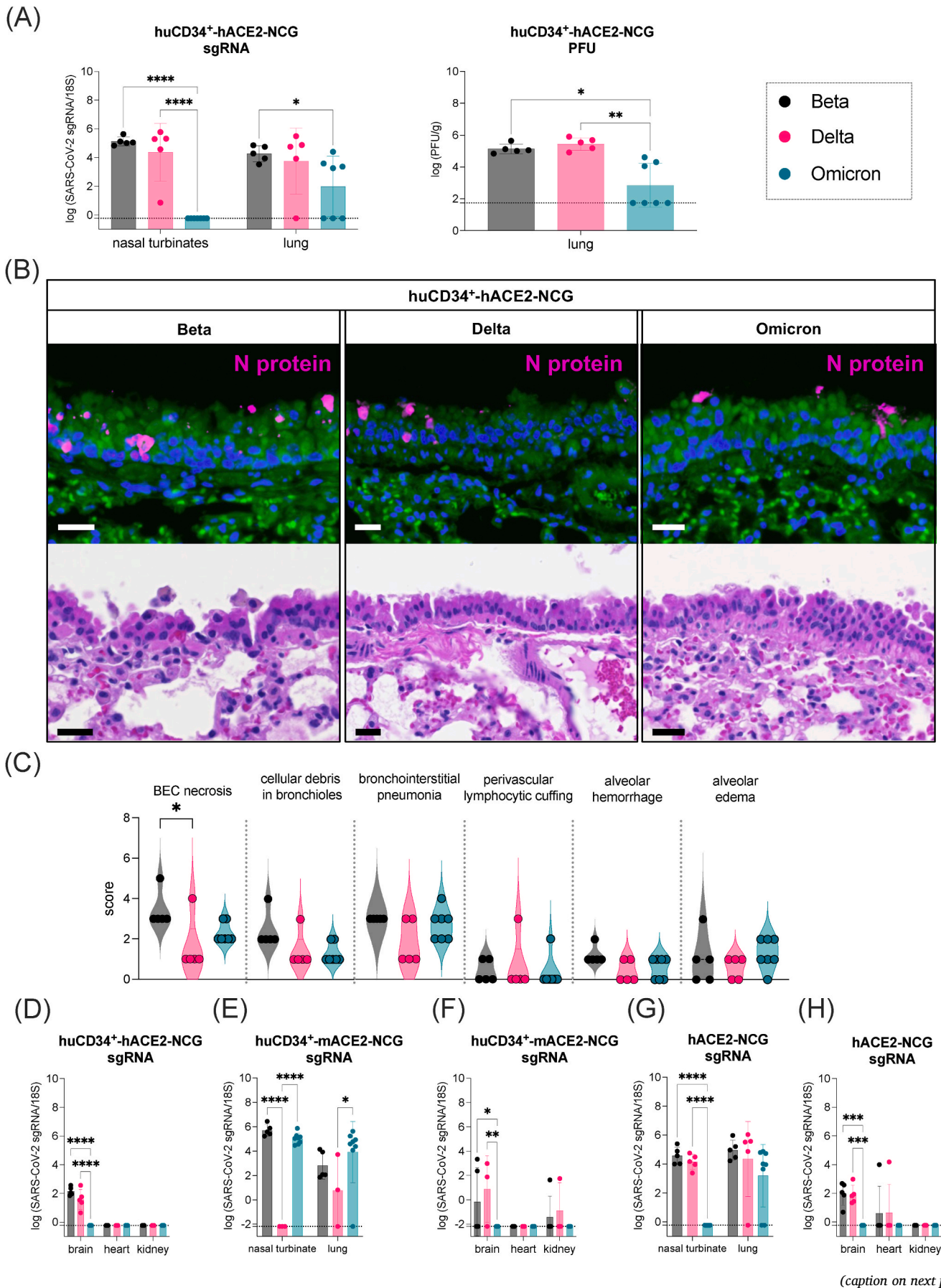


**Fig. 1.** SARS-CoV-2 Beta (B.1.351) and Delta (B.1.617.2), but not Omicron (B.1.1.529 BA.2) infect the brain of NCG mice regardless of h/mACE2 expression or huCD34<sup>+</sup> immune reconstitution.

NCG mice harboring human ACE2 (hACE2-NCG) or mouse ACE2 (mACE2-NCG) were reconstituted with human CD34<sup>+</sup> cells and then infected intranasally with 10<sup>4</sup> PFU SARS-CoV-2 B.1.351 (n = 5, 5, 5 for huCD34<sup>+</sup>-hACE2-NCG, huCD34<sup>+</sup>-mACE2-NCG, hACE2-NCG mice, respectively), B.1.617.2 (n = 5, 3, 5 respectively), or B.1.1.529 BA.2 (n = 7, 8, 8, respectively) and tissues were harvested on day 3 post-infection. (A) qRT-PCR analysis of SARS-CoV-2 7a subgenomic RNA (left) and Vero E6 plaque assay (right) of nasal turbinate and lung samples from huCD34<sup>+</sup>-hACE2-NCG mice. (B, upper row) Representative immunofluorescence microscopy images showing SARS-CoV-2 N protein localization (magenta) in bronchiolar epithelial cells (BEC) in infected huCD34<sup>+</sup>-hACE2-NCG mice. (B, lower row) Representative H&E images from adjacent or nearby lung sections, demonstrating morphologic changes. Scale bars, 20 μm. (C) Violin plots of histopathologic scores for six criteria of lung injury in individual mice. (D) qRT-PCR analysis of SARS-CoV-2 7a subgenomic RNA in brain, heart, and kidney samples from huCD34<sup>+</sup>-hACE2-NCG mice. (E) qRT-PCR analysis of SARS-CoV-2 7a subgenomic RNA in nasal turbinate and lung samples from huCD34<sup>+</sup>-mACE2-NCG mice. (F) qRT-PCR analysis of SARS-CoV-2 7a subgenomic RNA in brain, heart, and kidney samples from huCD34<sup>+</sup>-mACE2-NCG mice. (G) qRT-PCR analysis of SARS-CoV-2 7a subgenomic RNA in nasal turbinate and lung samples from hACE2-NCG mice. (H) qRT-PCR analysis of SARS-CoV-2 7a subgenomic RNA in brain, heart, and kidney samples from hACE2-NCG mice. Data in (A) and (D) through (H) are presented as the mean ± SD. Symbols represent individual mice. \*p < 0.05, \*\*p < 0.01, \*\*\*p < 0.001, \*\*\*\*p < 0.0001 by Dunnett's multiple comparison test, except for (A) plaque assay and (C), which were analyzed by the nonparametric Kruskal–Wallis test.

quantitatively and in localization between Beta, Delta, and Omicron, we next examined the types of lung injury induced by each VOC. Lung sections from huCD34<sup>+</sup>-hACE2-NCG mice at day 3 p.i. (sections adjacent or near to those used for IF) were stained with H&E and examined by a board-certified pathologist blinded to groupings and prior results (Fig. 1B). In addition, scores were assigned to 10 of 37 previously described criteria of histopathologic injury (Gruber et al., 2020), including BEC necrosis and bronchiointerstitial pneumonia (Fig. 1C). Consistent with the predominant localization of N protein to BECs, we found that histopathologic damage caused by Beta, Delta, and Omicron infection was centered specifically around infected bronchioles. Although the degree and type of injury was similar in the lungs of mice infected with each VOC, BEC necrosis was significantly higher in Beta-infected than Delta-infected lungs (Fig. 1C). However, BEC necrosis was not significantly different in comparisons of Beta-vs Omicron-infected lungs and Delta-vs Omicron-infected lungs. Necrotizing bronchiolitis observed in some mice was variably characterized by luminal cellular/nuclear debris or rounded epithelial cells with excessively eosinophilic cytoplasm and shrunken nuclei with condensed chromatin (Fig. 1B). Other lesions (data not shown) included mild bronchus-associated lymphoid tissue hyperplasia (increased small round cells with scant cytoplasm and round, dark blue nuclei), interstitial pneumonia (lymphohistiocytic expansion of the alveolar septae with increased numbers of small round cells with scant cytoplasm and round, dark blue nuclei and large round mononuclear cell with round to reniform nucleus), and pulmonary edema (homogenous pink material in alveolar air spaces). Taken together, these findings indicate that despite the reduced level of Omicron infection in the lungs of infected huCD34<sup>+</sup>-hACE2-NCG mice, all three SARS-CoV-2 lineages induced mostly similar types and degrees of pulmonary injury at day 3 p.i.

### 2.3. SARS-CoV-2 Beta and Delta, but not Omicron, replicate in the brain of immunodeficient and immune-reconstituted mice expressing mouse or human ACE2

Having observed that Beta, Delta, and Omicron display differing patterns of infection in the upper respiratory tract, we also measured infection in the brain, heart, and kidneys of huCD34<sup>+</sup>-hACE2-NCG mice. Measurement of SARS-CoV-2 sgRNA at 3 day p.i. showed that Beta and Delta productively infected the brain, whereas viral sgRNA was undetectable in the brain of Omicron-infected mice, and none of the VOCs exhibited significant infection of the heart or kidney (Fig. 1D). This result is consistent with the inability of Omicron to infect the nasal cavity, which may be a route to ascending brain infection. To determine whether mACE2 may enable Omicron infection of these tissues, we inoculated huCD34<sup>+</sup>-mACE2-NCG mice i.n. with 10<sup>4</sup> PFU of Beta, Delta, or Omicron and then examined viral sgRNA levels in tissues at day 3 p.i. Indeed, expression of mACE2 permitted Omicron to productively infect both the nasal turbinates and lungs (Fig. 1E); however, mACE2 expression did not enable infection of the brain (Fig. 1F). Of note, mACE2 expression suppressed the ability of Delta to infect the nasal

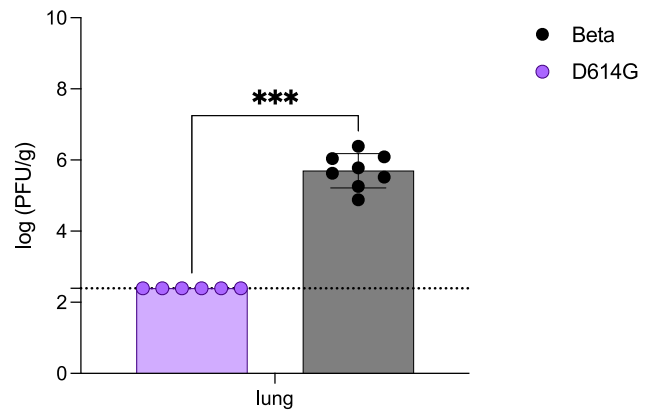
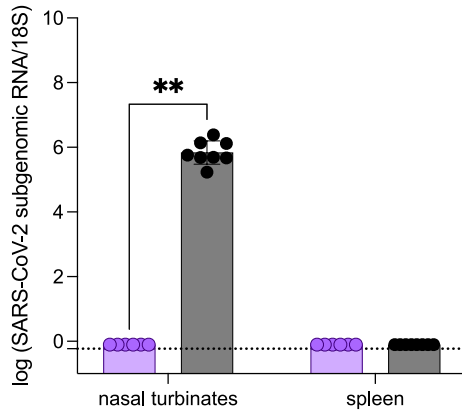
turbinates and lungs (Fig. 1E). This may be due to the presence of the N501Y mutation that permits binding of the Spike protein to mACE2 and is carried by Beta and Omicron variants but not by Delta (Montagutelli et al., 2021; Rathnasinghe et al., 2021; Chen et al., 2021). Interestingly, however, expression of mACE2 did not appear to have an impact on the ability of Delta to infect the brain (Fig. 1F).

Because both huCD34<sup>+</sup>-hACE2-NCG and huCD34<sup>+</sup>-mACE2-NCG mice are reconstituted with human immune cells, we also determined whether a functioning immune system influences SARS-CoV-2 neurotropism. We examined SARS-CoV-2 sgRNA levels in tissues from unreconstituted hACE2-NCG mice at 3 days after i.n. inoculation with Beta, Delta, and Omicron. We found that the tissue infection pattern by all three SARS-CoV-2 VOCs were virtually identical in hACE2-NCG mice to those observed in huCD34<sup>+</sup>-hACE2-NCG mice. Specifically, Beta and Delta sgRNA was readily detectable in the nasal turbinates, lungs, and brains of hACE2-NCG mice, whereas productive Omicron infection was observed only in the lungs (Fig. 1G and H). Taken together, these data indicate that expression of human or mouse ACE2 has a profound effect on the ability of SARS-CoV-2 Delta and Omicron to infect the respiratory tract, but not the brain, and additionally that the pattern of SARS-CoV-2 infection at 3 days p.i. appears to be unaffected by the presence or absence of a functional immune system.

### 2.4. SARS-CoV-2 D614G and Beta induce comparable human CD4<sup>+</sup> and CD8<sup>+</sup> T cell responses in the lungs and spleens of huCD34<sup>+</sup>-mACE2-NCG mice

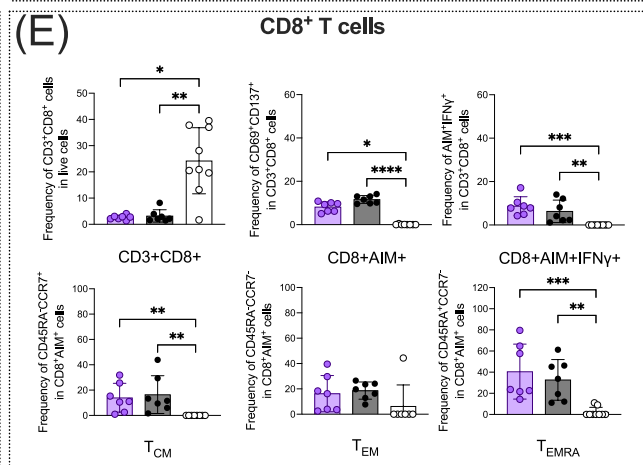
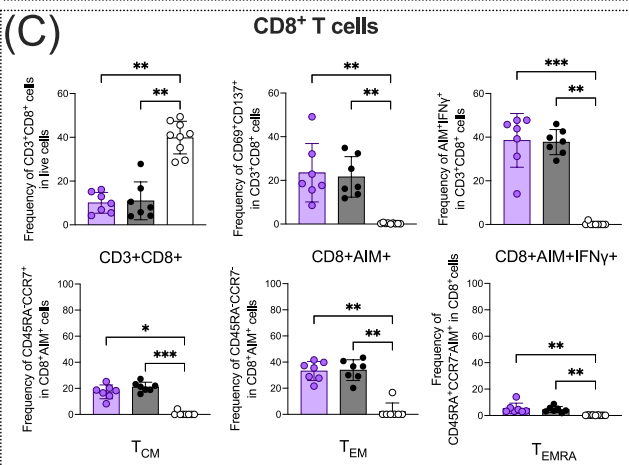
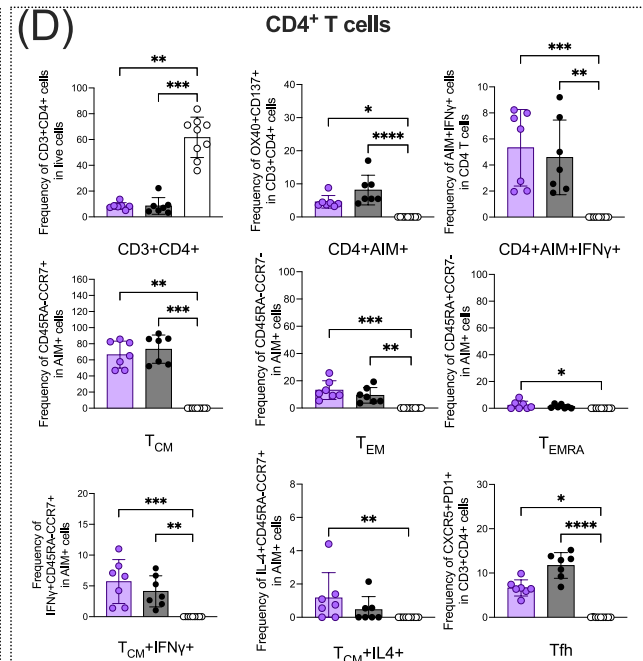
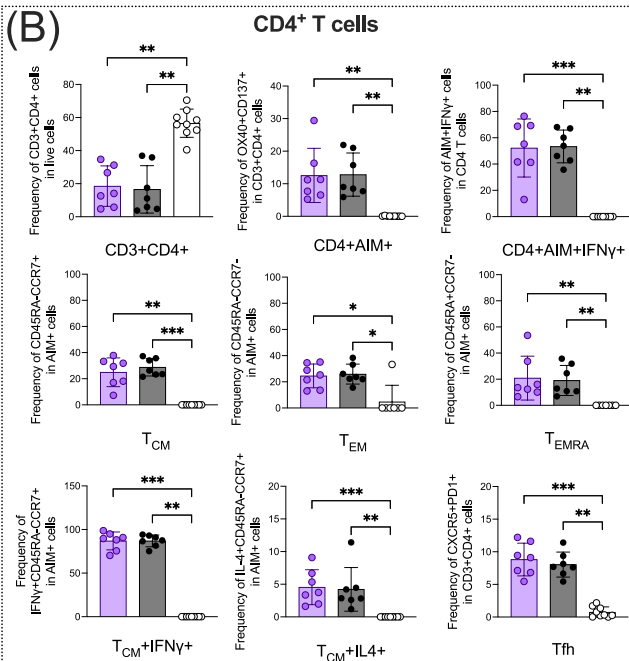
The observation that Omicron does not infect the brains of hACE2-NCG or huCD34<sup>+</sup>-hACE2-NCG mice raises two important questions: first, does exposure to SARS-CoV-2 induce a human immune response in the huCD34<sup>+</sup>-reconstituted mice? And second, if so, does the response depend on the level of detectable tissue infection? To address these questions, we performed an independent comprehensive assessment of the human immune response in huCD34<sup>+</sup>-mACE2-NCG mice infected either with Beta, which we showed replicates well in the respiratory tract and brain of these mice (Fig. 1A and D) or with D614G, an ancestral SARS-CoV-2 strain showing no evidence of replication in the respiratory tract of mice harboring native mACE2 (Winkler et al., 2022; Halfmann et al., 2022; Leist et al., 2020). Thus, comparing these strains permits us to evaluate whether the human immune response to SARS-CoV-2 is dependent on the level of detectable infection. As expected, inoculation of huCD34<sup>+</sup>-mACE2-NCG mice with 4 × 10<sup>4</sup> PFU of Beta resulted in readily detectable sgRNA and infectious virus in the nasal turbinates and lungs, respectively; whereas this was not observed with the same dose of D614G (Fig. 2A). To examine the immune response, splenocytes and lung cells were prepared from organs collected at 8 days p.i. and stimulated *in vitro* with a megapool of HLA class I and II SARS-CoV-2 Spike peptides for 24 h. Beta- or D614G-specific CD4<sup>+</sup> T cell, CD8<sup>+</sup> T cell, and B cell responses were then evaluated quantitatively and qualitatively by staining with antibodies against phenotypic markers, activation-induced markers (AIM), and cytokines followed by live-cell flow cytometry. The

(A)



(Spleen)

(Lung)



● D614G ● Beta ○ naïve

(caption on next page)

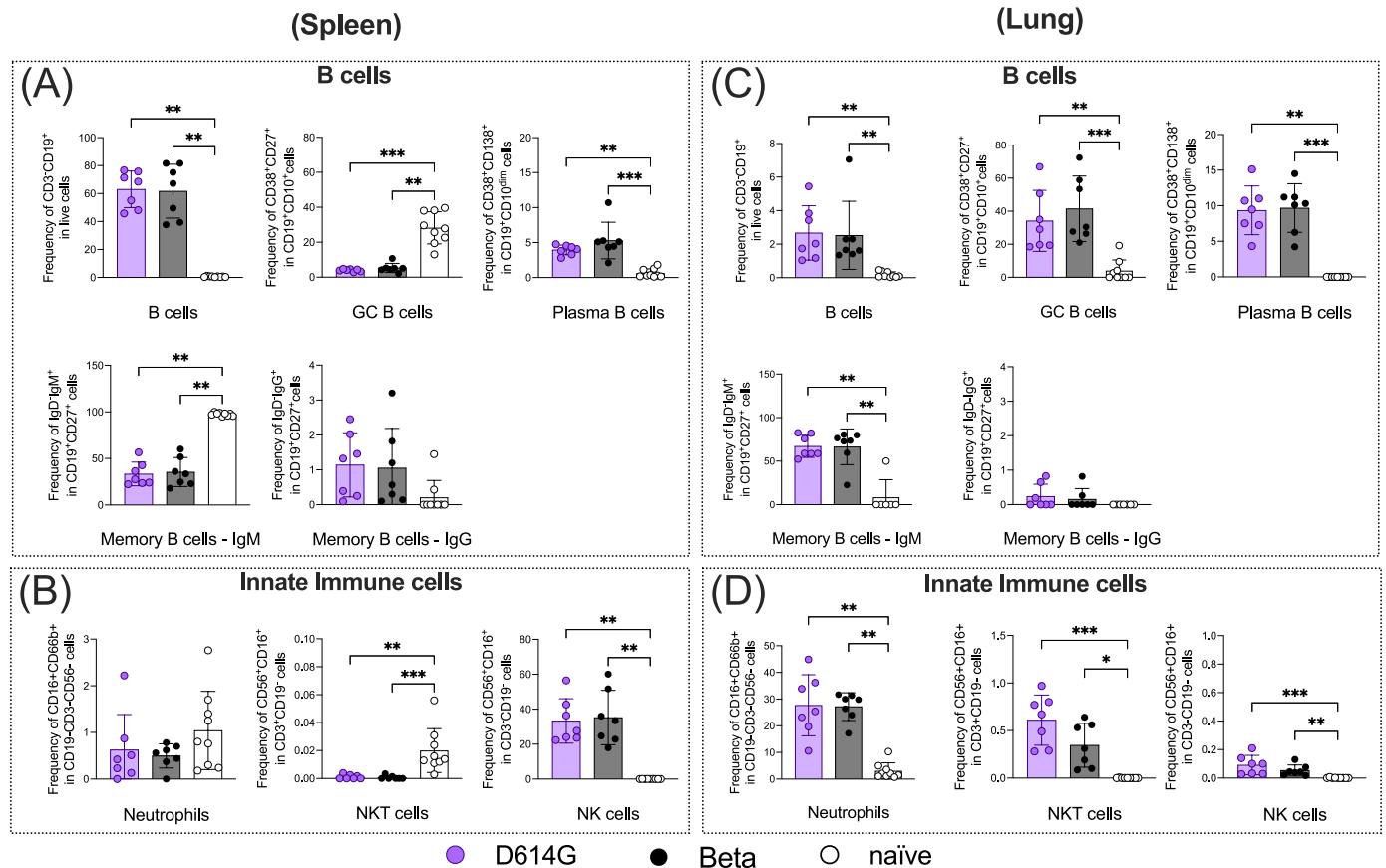
**Fig. 2.** Human T cell responses to SARS-CoV-2 D614G and B.1.351 in the spleens and lungs of huCD34<sup>+</sup>-mACE2-NGC mice.

huCD34<sup>+</sup>-mACE2-NGC mice were infected intranasally with  $4 \times 10^4$  PFU of SARS-CoV-2 D614G or B.1.351. (A) Nasal turbinates and lungs were collected from mice (D614G n = 6, B.1.351 n = 8) at day 3 post-infection for qRT-PCR analysis of SARS-CoV-2 7a subgenomic RNA and Vero E6 plaque assay. (B–E) Splenocytes (B, C) or lung cells (D, E) were prepared from infected mice or naïve mice (n = 9) at 8 days post-infection, stimulated for 24 h with a megapool of HLA class I and II SARS-CoV-2 Spike peptides, and then subjected to flow cytometry for evaluation of the percentage of CD4<sup>+</sup> (B, D) and CD8<sup>+</sup> (C, E) T cell subpopulations, including total CD3<sup>+</sup>CD4<sup>+</sup> T cells, activated (OX40<sup>+</sup>CD137<sup>+</sup> [AIM<sup>+</sup>]) CD4<sup>+</sup> T cells, IFN $\gamma$ -producing AIM<sup>+</sup>CD4<sup>+</sup> cells, central memory (T<sub>CM</sub>) AIM<sup>+</sup>CD4<sup>+</sup> cells, effector memory (T<sub>EM</sub>) AIM<sup>+</sup>CD4<sup>+</sup> cells, terminally differentiated effector memory (T<sub>EMRA</sub>) AIM<sup>+</sup>CD4<sup>+</sup> cells, IFN $\gamma$ -producing T<sub>CM</sub> AIM<sup>+</sup>CD4<sup>+</sup> cells, IL-4-producing T<sub>CM</sub> AIM<sup>+</sup>CD4<sup>+</sup> cells, T follicular helper (Tfh) CD4<sup>+</sup> cells, total CD8<sup>+</sup> T cells, activated (CD69<sup>+</sup>CD137<sup>+</sup> [AIM<sup>+</sup>]) CD8<sup>+</sup> T cells, IFN $\gamma$ -producing AIM<sup>+</sup>CD8<sup>+</sup> T cells, T<sub>CM</sub> AIM<sup>+</sup>CD8<sup>+</sup> T cells, T<sub>EM</sub> AIM<sup>+</sup>CD8<sup>+</sup> T cells, and T<sub>EMRA</sub> AIM<sup>+</sup>CD8<sup>+</sup> T cells. Purple circles, black circles, and open circles represent D614G-infected, B.1.351-infected, and naïve mice, respectively. Data are presented as the mean  $\pm$  SD. Symbols represent individual mice. \*p < 0.05, \*\*p < 0.01, \*\*\*p < 0.001, \*\*\*\*p < 0.0001 by the Mann–Whitney test (A) and the nonparametric Kruskal–Wallis test (B–E).

frequencies of CD4<sup>+</sup> T cells (Fig. 2B) and CD8<sup>+</sup> T cells (Fig. 2C) in the spleen were significantly decreased in D614G- or Beta-infected huCD34<sup>+</sup>-mACE2-NGC mice compared with naïve mice, and no significant differences were observed between D614G- and Beta-infected mice. Similarly, no significant variant-specific differences were detected in the frequencies of activated (OX40<sup>+</sup>CD137<sup>+</sup>) CD4<sup>+</sup> T cells, activated (CD69<sup>+</sup>CD137<sup>+</sup>) CD8<sup>+</sup> T cells, or IFN- $\gamma$ -secreting activated CD4<sup>+</sup> or CD8<sup>+</sup> T cells (Fig. 2B and C), despite the fact that productive virus infection was only observed with the Beta strain. Moreover, expansion of SARS-CoV-2-reactive central memory (T<sub>CM</sub>) cells, cytokine-secreting T<sub>CM</sub> cells, effector memory (T<sub>EM</sub>) cells, and T<sub>EMRA</sub> cells was comparable in both the CD4<sup>+</sup> and CD8<sup>+</sup> T cell compartments in mice infected with D614G or B.1.351 (Fig. 2B and C, and S1). Thus, although there were minor variant-specific differences in the frequencies of some cell subsets, overall, the human T cell immune response in the spleen was remarkably similar in huCD34<sup>+</sup>-mACE2-NGC mice after i.n. exposure to

Beta, a strain that robustly replicates in the upper and lower respiratory tract, or with D614G, a strain that exhibits no detectable infection.

We performed a similar analysis of lung cells from Beta- or D614G-infected huCD34<sup>+</sup>-mACE2-NGC mice stimulated *in vitro* with SARS-CoV-2 Spike peptides, as described above (Fig. S2). Consistent with the results for splenocytes, the frequencies of both CD4<sup>+</sup> (Fig. 2D) and CD8<sup>+</sup> (Fig. 2E) T cells, but not the absolute cell numbers (Figs. S3A–S3C), in the lungs were significantly lower in SARS-CoV-2-infected mice compared with naïve mice, and the responses in mice infected with Beta or D614G did not differ significantly. Also similar to the splenocyte responses, lung cells from D614G- and Beta-infected mice did not differ in the frequencies of activated (AIM<sup>+</sup>) CD4<sup>+</sup> or CD8<sup>+</sup> T cells, IFN $\gamma$ -producing AIM<sup>+</sup> cells, T<sub>CM</sub> cells, T<sub>EM</sub> cells, T<sub>EMRA</sub> cells, IFN- $\gamma$ -producing and IL-4-producing CD4<sup>+</sup> T<sub>CM</sub> cells, or Tfh cells (Fig. 2D and E).

**Fig. 3.** Human B cell and innate immune cell responses to SARS-CoV-2 D614G and B.1.351 variants in the spleens and lungs of HuCD34<sup>+</sup>-mACE2-NGC mice.

HuCD34<sup>+</sup>-mACE2-NGC mice were infected intranasally with  $4 \times 10^4$  PFU of SARS-CoV-2 D614G (n = 7) or B.1.351 (n = 7) for 8 days. Splenocytes (A, B) and lung cells (C, D) of infected and naïve (n = 9) mice were prepared, stained, and subjected to flow cytometry for evaluation of the percentages of B cells (A, C) and innate immune cell populations (B, D). Purple circles, black circles, and open circles represent D614G-infected, B.1.351-infected, and naïve mice, respectively. Data are presented as the mean  $\pm$  SD. \*p < 0.05, \*\*p < 0.01, \*\*\*p < 0.001, \*\*\*\*p < 0.0001 by the nonparametric Kruskal–Wallis test.

### 2.5. SARS-CoV-2 D614G and Beta induce similar humanized B cell responses but distinct IgM responses in huCD34<sup>+</sup>-mACE2-NGC mice

To determine whether i.n. exposure to D614G or Beta also elicited comparable human B cell responses, we analyzed CD19<sup>+</sup> B lymphocytes, plasma cells, and IgG<sup>+</sup> memory B cells in the spleens of infected huCD34<sup>+</sup>-mACE2-NGC mice (Fig. 3A). These three B cell subpopulations were similarly expanded in D614G- and B.1.351-infected mice compared with naïve mice, whereas the germinal center (GC) B cell and IgM<sup>+</sup> memory B cell (Fig. 3A) pools were decreased by infection with the two SARS-CoV-2 strains to a similar extent. Interestingly, we observed several differences between the spleen and lung cells of infected mice with respect to expansion vs contraction of B cell subpopulations (Fig. 3A vs 3C). Lung CD19<sup>+</sup> B cells and plasma cells (Fig. 3C) were expanded similarly in mice infected with D614G and Beta compared with naïve mice; however, GC B cells and IgM<sup>+</sup> memory B cells in the lungs (Fig. 3C) were both significantly expanded in SARS-CoV-2-infected mice compared with naïve mice, which was the opposite trend to that seen in the same cell populations in the spleen (Fig. 3A). Moreover, whereas spleen memory IgG<sup>+</sup> B cells underwent expansion upon exposure to Beta or D614G, the same cell population in the lungs was unaffected by SARS-CoV-2 exposure (Fig. 3A vs 3C). We also observed no significant differences between the B cell responses in Beta- and D614G-infected mice, as was also observed with spleen cells. Although we did not detect SARS-CoV-2 Spike protein-specific human IgG in the sera of Beta- or D614G-infected mice, serum levels of anti-Spike human IgM were significantly higher in Beta-infected mice compared with D614G-infected mice (Fig. S4), which is in line with the higher viral load observed in B.1.351-infected animals. Taken together, these results demonstrate that mucosal exposure to SARS-CoV-2, whether or not that results in detectable infection of the respiratory tract, was sufficient to elicit antigen-specific T cell and B cell responses in the lungs and spleens of huCD34<sup>+</sup>-mACE2-NGC mice.

### 2.6. Expansion of NKT cells, but not of other innate immune cell populations, differs between D614G- and B.1.351-infected huCD34<sup>+</sup>-mACE2-NGC mice

Because Beta, but not D614G, replication was detected in the respiratory tract of huCD34<sup>+</sup>-mACE2-NGC mice on day 3 p.i. (Fig. 2A) and the innate immune response plays a vital role in early antiviral immunity, we next examined the numbers and frequencies of neutrophils, NK cells, and NKT cells in the spleens and lungs of the same mice as examined above. NKT cells were defined here as CD56<sup>+</sup> T lymphocytes, thus distinguishing them from CD56<sup>-</sup> CD1d-reactive invariant NKT cells. Notably, the frequency of neutrophils was reduced in the spleens (Fig. 3B) but massively increased in the lungs (Fig. 3D) of both Beta- and D614G-infected mice compared with naïve mice, whereas the frequency of NK cells was markedly increased in the spleen and modestly increased in the lungs of infected mice compared with naïve mice (Fig. 3B vs 3D). The frequency (Fig. 3D) and absolute number (Fig. S3D) of NKT cells were both significantly increased in the lungs, but decreased in the spleens, of Beta- and D614G-infected mice compared with naïve mice. Although speculative, these results raise the possibility that NKT cells may play a role in preventing lung infection by the D614G variant. These analyses indicate that mucosal exposure to D614G and Beta strains can activate innate and adaptive human immune responses in huCD34<sup>+</sup>-mACE2-NGC mice within 8 days of infection. Overall, the human immune cell responses to both strains were remarkably similar, with the only variant-specific differences detected being a higher serum Spike protein-specific IgM level in response to Beta.

## 3. Discussion

Mouse models of SARS-CoV-2 infection are important tools for studying the virus effects on the brain, but little is known about the

neurotropism of different VOCs or whether that is influenced by the antiviral immune response. In this study, we sought to determine the relative ability of SARS-CoV-2 Beta, Delta, and Omicron to infect the brains of triple-immunodeficient NCG mice expressing hACE2 or native mACE2 with or without huCD34<sup>+</sup> engraftment. Our results provide several important insights into the use of mouse models for studying specific aspects of tissue tropism and the human immune response to SARS-CoV-2 VOCs. Most notably, we found that i.n. inoculation of Omicron, unlike Beta or Delta, failed to result in detectable infection of the brain, regardless of whether the SARS-CoV-2 receptor expressed was mACE2 or hACE2 or whether the mice had a functioning immune system. Our results suggest that the failure of Omicron to infect the brain was not due to an inability to bind to the cellular SARS-CoV-2 receptor or to clearance via an immune response occurring before day 3 p.i., the time at which tissue infection was evaluated. In addition to binding to entry receptors that mediate delivery of the viral genome into the cytoplasm, tissue and cell permissiveness to viral infection is the result of multiple factors. Omicron may not express viral structures that enable attachment to appropriate surface receptors (eg, C type lectins, glycosaminoglycans, and proteoglycans) or plasma membrane fusion/endocytosis to allow entry into the diverse cells of the CNS (Jackson et al., 2022). Omicron infection also may not sufficiently disrupt the blood-brain-barrier to allow hematogenous infection of the brain. Thus, modeling of the neurologic sequelae of SARS-CoV-2 infection should take into consideration the capacity of the specific VOC to recapitulate neurotropism. The results of the present study, which are supported in part by the findings that Omicron exhibits reduced neurotropism compared with other strains in immunocompetent hamsters (Bauer et al., 2022; Mohandas et al., 2022; Armando et al., 2022) and K18-ACE2 mice (Chan et al., 2022; Seehusen et al., 2022; Natekar et al., 2022), indicate that Omicron is likely not a suitable strain for studies of the effects of direct SARS-CoV-2 infection of the brain in the most common mouse models. Based on a study showing that genomic RNA was detected in brains of RAG2 knockout or cyclophosphamide-treated hamsters following infection with SARS-CoV-2 USA-WA-1/2020 (Brocato et al., 2020), hamsters with deficient adaptive immune components may support SARS-CoV-2 infection of the brain. Thus, novel SARS-CoV-2 lineages that emerge in the future should be carefully assessed for tissue tropism in each animal model.

Although SARS-CoV-2 has been detected in autopsied brain tissue from infected patients, we cannot assume that all neurocognitive aspects of COVID-19 are due to direct brain infection by the virus. Indirect mechanisms that could affect the brain include inflammation, migration of non-infectious viral proteins into the brain, and alterations in blood and CSF circulation. Although not an ideal SARS-CoV-2 lineage for modeling direct infection of the brain, Omicron could serve as an excellent control for extracranial causes of neurocognitive dysfunction, given its ability to infect and cause damage to the respiratory tract.

Studies in both humans and animal models have shown that ascending infection of SARS-CoV-2 from the nose to the olfactory region is at least one component of the pathogenesis of brain infection (Rhea et al., 2021; Khan et al., 2021, 2022; Song et al., 2021; Meinhardt et al., 2021; Zheng et al., 2021). In our study, we did not observe Omicron brain infection in any of the mouse strains assessed, even though highly productive infection of the nasal turbinates was observed in huCD34<sup>+</sup>-mACE2-NGC mice. Studies of infected patient tissues obtained at autopsy before the emergence of Omicron showed that SARS-CoV-2 lineages could infect at least 34 human cell populations (ea, 2021); thus it was assumed that SARS-CoV-2 was a pantropic virus. In addition to the olfactory route, ascension of SARS-CoV-2 to the brain could occur via other cranial nerves or the vagus nerve, intracellular trafficking, and hematogenous infection breaching the blood-brain barrier (Meinhardt et al., 2021; Cantuti-Castelvetri et al., 2020).

In addition to the neurotropism findings, our study showed that the lungs of huCD34<sup>+</sup>-hACE2-NGC, huCD34<sup>+</sup>-mACE2-NGC, and hACE2-NGC mice are permissive to Omicron infection. Human-reconstituted

immunodeficient mice have some advantages over immunocompetent mice for COVID studies. For example, the mice can be engrafted with cells from the same donor under highly controlled conditions, and the responses of a diverse population of human immune cells can be explored. Moreover, the mice can be reconstituted with cells selected for particular donor characteristics, such as ethnicity, gender, and pre-existing immunity to SARS-CoV-2 VOCs, which could be of great help in deciphering genetic and epigenetic influences on the immune response that affect susceptibility to infection by SARS-CoV-2 lineages, as well as on the severity of disease and response to therapy. Of note, the cord blood-derived cells used for reconstitution of our mice undergo apheresis prior to engraftment, thus eliminating concerns based on the high proportion of humans who now have infection- or vaccination-elicited immunity to various SARS-CoV-2 lineages. Although foeto-maternal chimerism is a possible mechanism by which maternal SARS-CoV-2-exposed T cells (Hahn et al., 2019) could be present in cord blood, such cells would be extremely rare and expected to have a negligible impact on the overall SARS-CoV-2 infectivity and immune responses in these mice.

The observation that D614G and Beta elicited virtually identical humanized T cell, B cell, and innate immune cell responses, despite the lack of detectable D614G replication, is also striking. It is possible that by sampling on day 3 p.i., we may have missed an earlier or later transient burst of D614G replication. Nevertheless, our data demonstrate that i.n. inoculation of D614G without overt pulmonary infection was sufficient to enable viral uptake and antigen presentation, resulting in an immune response to D614G in both the lungs and spleen by day 8 p.i. This is in-line with clinical studies suggesting that (i) cross-reactive memory T cells allowed healthcare workers to abort SARS-CoV-2 infection, resulting in repeatedly negative PCR and serology testing for SARS-CoV-2 (Swadling et al., 2022), and (ii) individuals with even asymptomatic or mild COVID-19 exhibit a robust T-cell immunity response (Sekine et al., 2020). Our finding is also consistent with studies demonstrating that antigen-specific splenic CD4<sup>+</sup> T cells are elicited following mucosal administration of adenovirus-vectored trivalent vaccine (Afkhami et al., 2022), and that nasal administration of either unadjuvanted Spike (Mao et al., 2022) or adenovirus-vectored Spike (Lapiente et al., 2021) vaccine boosters stimulate systemic immunity. In a mouse model of influenza virus A infection, lung dendritic cells were found to migrate to the spleen and effectively prime T cells (Jenkins et al., 2021). Thus, we hypothesize that the observed T cell response to D614G antigens in our study reflects similar trafficking and antigen presentation events.

In our study, we found significantly decreased frequencies of CD4<sup>+</sup> and CD8<sup>+</sup> T cells in the lungs and spleens of SARS-CoV-2-infected mice compared with naïve mice. Previous work showed that about 80% of acute-phase SARS patients become lymphopenic within the first 2 weeks after disease onset (Wang et al., 2020a). Similarly, 34% of patients with laboratory-confirmed Middle East respiratory syndrome exhibited lymphopenia (Wang et al., 2020a). Decreased numbers of circulating B cells and CD3<sup>+</sup>, CD4<sup>+</sup>, and CD8<sup>+</sup> T cells have also been documented within 23 days of symptom onset in 93% of a cohort of patients with PCR-confirmed COVID-19 (Mazzoni et al., 2020), and lymphopenia has been reported to correlate with disease severity in another cohort of SARS-CoV-2 patients (Tan et al., 2020). Our results are consistent with these findings and show that infection with either D614G or B.1.351 results in lymphocyte depletion in huCD34<sup>+</sup>-NCG mice.

Despite lymphopenia and the absence of HLA, mice inoculated with either D614G or B.1.351 variants generated robust Spike protein-specific CD4<sup>+</sup> and CD8<sup>+</sup> T cell responses in huCD34<sup>+</sup>-NCG mice, which is in agreement with human studies (Tarke et al., 2021). Our finding that the SARS-CoV-2-specific humanized T cell response consisted predominantly of Th1, Tfh, and T<sub>CM</sub>, T<sub>EM</sub>, and T<sub>EMRA</sub> CD8<sup>+</sup> T cells is also consistent with studies in humans (Rydzynski Moderbacher et al., 2020). The overall magnitude, phenotype, and functionality of these antigen-specific T cells were similar in D614G- and B.1.351-infected

mice. Future studies examining additional variants and different viral challenge doses and time points after infection may uncover more subtle differences in the T cell responses to variants. Overall, our results suggest that T cell responses to D614G and B.1.351 are likely to be similar in humans during acute SARS-CoV-2 infection.

NKT cells are crucial components of the innate immune response against viral infection (Khan and Khan, 2021). In addition to their ability to directly lyse virally infected cells, NKT cells can modulate innate (dendritic cells, macrophages, and NK cells) and adaptive (T and B cells) *via* secretion of Th1 and Th2 cytokines, including IFN $\gamma$  and IL-4 (Juno et al., 2012; Gaya et al., 2018). A dramatic and early loss of circulating NKT cells has also been reported in COVID-19 patients (Kreutmair et al., 2021), and the loss was shown to correlate with severe COVID-19 pneumonia (Zingaropoli et al., 2021). We also observed that the NKT cell population was considerably reduced in the spleens but was expanded in the lungs of SARS-CoV-2-infected mice compared with naïve mice. Thus, we speculate that NKT cell responses may represent an important immune checkpoint that limits SARS-CoV-2 infection of the lungs. Finally, we note that hACE2-NCG mice represent a potentially powerful tool for SARS-CoV-2 studies given that it is a permissive host for Beta, Delta, and Omicron pulmonary infection and can be engrafted with human immune cells and other tissues. Because the median incubation period of SARS-CoV-2 is 4–5 days and the median time from symptom onset to hospitalization is 8–11 days (Wang et al., 2020b, 2021; Yang et al., 2020; Zhou et al., 2020), we still know relatively little about the human cellular immunologic response during the first 2 weeks after SARS-CoV-2 infection, which is a period when key events leading to morbidity and or mortality are accruing.

### 3.1. Study limitations

Although mice harboring human immune cells are increasingly utilized for preclinical immuno-oncology studies (Guil-Luna et al., 2021), they cannot completely recapitulate the human T and B cell responses for reasons that include the absence of HLA (NCG mice are MHC haplotype H2<sup>87</sup>). In addition, human immune cells engrafted into immunodeficient mice exhibit certain functional impairments, such as IgG production, due to the absence of human cytokines and trophic factors (Kenney et al., 2022; Fu et al., 2021; Shang et al., 2021; Wahl et al., 2021; Sefik et al., 2021, 2022). Thus the immune cell responses against SARS-CoV-2 in our study must be interpreted in this light. In addition, our neurotropism studies measured viral burden at a single time point (day 3 p.i). Addition of later time points may have been able to reveal brain infection in the neurotropism experiments, and earlier time points may have detected transient burst of D614G replication. Finally, while transgenic mouse models of COVID-19 continue to be refined, mice cannot be expected to completely recapitulate the pathogenic events leading to human brain infection.

### Declaration of interests

SF and JR are employed by Charles River Laboratories, Inc. AS is a consultant for Gritstone, Flow Pharma, Arcturus, Immunoscope, CellCarta, Oxford Immunotech, and Avalia. The remaining authors declare no competing interests.

### Author summary

COVID-19 is known to cause brain-related symptoms, including headache and brain fog, but the relative ability of SARS-CoV-2 variants to infect the brain is unclear. Here, we compared infection of the brain of immunodeficient mice and mice reconstituted with human immune cells by Omicron, Beta, and Delta variants. We found that Omicron uniquely failed to infect the brain in either mouse strain. These results indicate that modeling of COVID-related neurologic pathologies requires careful selection of an appropriate SARS-CoV-2 strain in the context of a specific

animal model.

### Author contributions

Conceptualization: Y-TW, KK, RA, SS. Investigation: Y-TW, KK, RA, ZM, SM, NA, KV, RM, SV, FSB, MN, CM, MZ, SA, JR, MK, DW, AS, KH, ES, SF, SS. Supervision: SS. Writing – original draft: Y-TW, KK, RA, SS. Writing – reviewing & editing: ZM, SM, NA, KV, RM, SV, FSB, MN, CM, MZ, SA, JR, MK, DW, AS, KH, ES, SF, KK, SS.

### Declaration of interests

SF and JR are employed by Charles River Laboratories, Inc. AS is a consultant for Gritstone, Flow Pharma, Arcturus, Immunoscope, CellCarta, Oxford Immunotech, and Avalia. The remaining authors declare no competing interests.

### Data availability

Data will be made available on request.

### Acknowledgements

This study was supported by Charles River Laboratories, Inc. SS and EOS were funded by NIH grant U19AI142790 and the Overton Family. DW and AS were funded by the NIH contract Nr. 75N9301900065. SM was supported by an imaging scientist grant from the Chan Zuckerberg Initiative. We would like to thank Ms. Angela Denn, Ms. Katarzyna Dobaczewska, and Mr. Brett Laffey for their excellent assistance with histology and immunostaining. Anti-SARS-CoV-2 antibodies for immunofluorescence were kindly provided by Genetex.

### Appendix A. Supplementary data

Supplementary data to this article can be found online at <https://doi.org/10.1016/j.antiviral.2023.105580>.

### References

- Afkhami, S., D'Agostino, M.R., Zhang, A., Stacey, H.D., Marzok, A., Kang, A., et al., 2022. Respiratory mucosal delivery of next-generation COVID-19 vaccine provides robust protection against both ancestral and variant strains of SARS-CoV-2. *e19*. Epub 2022/02/19 Cell 185 (5), 896–915. <https://doi.org/10.1016/j.cell.2022.02.005>. PubMed PMID: 35180381; PubMed Central PMCID: PMCPCMC8825346.
- Armando, F., Beythien, G., Kaiser, F.K., Allnoch, L., Heydemann, L., Rosiak, M., et al., 2022. SARS-CoV-2 Omicron variant causes mild pathology in the upper and lower respiratory tract of hamsters. *Nat. Commun.* 13 (1), 3519. <https://doi.org/10.1038/s41467-022-31200-y>.
- Bauer, L., Rissmann, M., Benavides, F.F.W., Leijten, L., Begeman, L., Kroeze, E.V., et al., 2022. Differences in neuroinflammation in the olfactory bulb between D614G, Delta and Omicron BA.1 SARS-CoV-2 variants in the hamster model. *bioRxiv*. <https://doi.org/10.1101/2022.03.24.485596>, 2022.03.24.485596.
- Bishop, C.R., Dumenil, T., Rawle, D.J., Le, T.T., Yan, K., Tang, B., et al., 2022. Mouse models of COVID-19 recapitulate inflammatory pathways rather than gene expression. *Epub 20220926 PLoS Pathog.* 18 (9), e1010867. <https://doi.org/10.1371/journal.ppat.1010867>. PubMed PMID: 36155667; PubMed Central PMCID: PMCPCMC9536645.
- Brocato, R.L., Principe, L.M., Kim, R.K., Zeng, X., Williams, J.A., Liu, Y., et al., 2020. Disruption of adaptive immunity enhances disease in SARS-CoV-2-infected Syrian hamsters. *J. Virol.* 94 (22) <https://doi.org/10.1128/JVI.01683-20> e01683-20.
- Cantuti-Castelvetri, L., Ojha, R., Pedro, L.D., Djannatian, M., Franz, J., Kuivanen, S., et al., 2020. Neuropilin-1 facilitates SARS-CoV-2 cell entry and infectivity. *Epub 20201020 Science* 370 (6518), 856–860. <https://doi.org/10.1126/science.abd2985>. PubMed PMID: 33082293; PubMed Central PMCID: PMCPCMC7857391.
- Cao, Y., Jian, F., Wang, J., Yu, Y., Song, W., Yisimayi, A., et al., 2022. Imprinted SARS-CoV-2 humoral immunity induces convergent Omicron RBD evolution, 2022.09.15.507787 *bioRxiv*. <https://doi.org/10.1101/2022.09.15.507787>.
- Chan, J.F.-W., Hu, B., Chai, Y., Shuai, H., Liu, H., Shi, J., et al., 2022. Virological features and pathogenicity of SARS-CoV-2 Omicron BA.2. *Cell Rep. Med.* 3 (9), 100743 <https://doi.org/10.1016/j.xcrm.2022.100743>.
- Chen, R.E., Winkler, E.S., Case, J.B., Aziati, I.D., Bricker, T.L., Joshi, A., et al., 2021. In vivo monoclonal antibody efficacy against SARS-CoV-2 variant strains. *Nature* 596 (7870), 103–108. <https://doi.org/10.1038/s41586-021-03720-y>.

- Crunfli, F., Carregari, V.C., Veras, F.P., Silva, L.S., Nogueira, M.H., Antunes, A., et al., 2022. Morphological, cellular, and molecular basis of brain infection in COVID-19 patients. *Epub 20220811 Proc. Natl. Acad. Sci. U. S. A.* 119 (35), e2200960119. <https://doi.org/10.1073/pnas.2200960119>. PubMed PMID: 35951647; PubMed Central PMCID: PMCPCMC9436354.
- Dangayach, N.S., Newcombe, V., Sonnerville, R., 2022. Acute neurologic complications of COVID-19 and postacute sequelae of COVID-19. *Epub 20220323 Crit. Care Clin.* 38 (3), 553–570. <https://doi.org/10.1016/j.ccc.2022.03.002>. PubMed PMID: 35667743; PubMed Central PMCID: PMCPCMC8940578.
- de Oliveira, L.G., de Souza Angelo, Y., Yamamoto, P., Carregari, V.C., Crunfli, F., Reis-de-Oliveira, G., et al., 2022. SARS-CoV-2 infection impacts carbon metabolism and depends on glutamine for replication in Syrian hamster astrocytes. *Epub 20220815 J. Neurochem.* 163 (2), 113–132. <https://doi.org/10.1111/jnc.15679>. PubMed PMID: 35880385; PubMed Central PMCID: PMCPCMC9350388.
- ea, Chertow, 2021. SARS-CoV-2 infection and persistence throughout the human body and brain. *Res Sq.* <https://doi.org/10.21203/rs.3.rs-1139035/v1>.
- Eberle, C., Rowe, J., Fiore, A., Mihalek, R., Festin, S., 2020. 199 Enhanced immune responses in human breast and colon cancer following checkpoint therapy in a CD34<sup>+</sup> stem cell humanized NCG (HuCD34NCG) mouse model. *J. Immunother. Cancer* 8 (Suppl. 3). <https://doi.org/10.1136/jitc-2020-SITC2020.0199>. A117-A.
- Elliott P, Eales O, Steyn N, Tang D, Bodinier B, Wang H, et al. Twin peaks: the Omicron SARS-CoV-2 BA.1 and BA.2 epidemics in England. *Science*. 376(6600):eabq4411. doi: 10.1126/science.abq4411.
- Fernández-Castañeda, A., Lu, P., Geraghty, A.C., Song, E., Lee, M.H., Wood, J., et al., 2022. Mild respiratory SARS-CoV-2 infection can cause multi-lineage cellular dysregulation and myelin loss in the brain. *Epub 20220110 bioRxiv*. <https://doi.org/10.1101/2022.01.07.475453>. PubMed PMID: 35043113; PubMed Central PMCID: PMCPCMC8764721.
- Focosi, D., McConnell, S., Casadevall, A., 2022. The Omicron variant of concern: diversification and convergent evolution in spike protein, and escape from anti-Spike monoclonal antibodies. *Epub 20221003 Drug Resist. Updates* 65, 100882. <https://doi.org/10.1016/j.drug.2022.100882>. PubMed PMID: 36260961; PubMed Central PMCID: PMCPCMC9528072.
- Fu, W., Wang, W., Yuan, L., Lin, Y., Huang, X., Chen, R., et al., 2021. A SCID mouse-human lung xenograft model of SARS-CoV-2 infection. *Epub 20210503 Theranostics* 11 (13), 6607–6615. <https://doi.org/10.7150/thno.58321>. PubMed PMID: 33995679; PubMed Central PMCID: PMCPCMC8120224.
- Fumagalli, V., Ravà, M., Marotta, D., Di Lucia, P., Laura, C., Sala, E., et al., 2022. Administration of aerosolized SARS-CoV-2 to K18-hACE2 mice uncouples respiratory infection from fatal neuroinvasion. *Epub 20220128 Sci. Immunol.* 7 (67), eabl9929. <https://doi.org/10.1126/sciimmunol.abl9929>. PubMed PMID: 34812647.
- Gaya, M., Barral, P., Burbage, M., Aggarwal, S., Montaner, B., Warren Navia, A., et al., 2018. Initiation of antiviral B cell immunity relies on innate signals from spatially positioned NKT cells. *Cell* 172 (3). <https://doi.org/10.1016/j.cell.2017.11.036>, 517–33.e20.
- Gruber, A.D., Osterrieder, N., Bertzbach, L.D., Vladimirova, D., Greuel, S., Ihlow, J., et al., 2020. Standardization of reporting criteria for lung pathology in SARS-CoV-2 infected hamsters: what matters? *Am. J. Respir. Cell Mol. Biol.* 63 (6), 856–859. <https://doi.org/10.1165/rcmb.2020-0280LE>. PubMed PMID: 32897757; PubMed Central PMCID: PMCPCMC7790148.
- Guil-Luna, S., Sedlik, C., Piaggio, E., 2021. Humanized mouse models to evaluate cancer immunotherapeutics. *Annu. Rev. Cell Biol.* 5 (1), 119–136. <https://doi.org/10.1146/annurev-cancerbio-050520-100526>.
- Hahn, S., Hasler, P., Vokalova, L., van Breda, S.V., Than, N.G., Hoesli, I.M., et al., 2019. Feto-maternal microchimerism: the pre-eclampsia conundrum. *Front. Immunol.* 10 <https://doi.org/10.3389/fimmu.2019.00659>.
- Halfmann, P.J., Iida, S., Iwatsuki-Horimoto, K., Maemura, T., Kiso, M., Scheaffer, S.M., et al., 2022. SARS-CoV-2 Omicron virus causes attenuated disease in mice and hamsters. *Nature* 603 (7902), 687–692. <https://doi.org/10.1038/s41586-022-04441-6>.
- Jackson, C.B., Farzan, M., Chen, B., Choe, H., 2022. Mechanisms of SARS-CoV-2 entry into cells. *Nat. Rev. Mol. Cell Biol.* 23 (1), 3–20. <https://doi.org/10.1038/s41580-021-00418-x>.
- Jenkins, M.M., Bachus, H., Botta, D., Schultz, M.D., Rosenberg, A.F., León, B., et al., 2021. Lung dendritic cells migrate to the spleen to prime long-lived TCF1(hi) memory CD8(+) T cell precursors after influenza infection. *Epub 2021/09/14 Sci. Immunol.* 6 (63), eabg6895. <https://doi.org/10.1126/sciimmunol.abg6895>. PubMed PMID: 34516781.
- Juno, J.A., Keynan, Y., Fowke, K.R., 2012. Invariant NKT cells: regulation and function during viral infection. *Epub 2012/08/24 PLoS Pathog.* 8 (8), e1002838. <https://doi.org/10.1371/journal.ppat.1002838>. PubMed PMID: 22916008; PubMed Central PMCID: PMCPCMC3420949.
- Kenney, D.J., O'Connell, A.K., Turcinovic, J., Montanaro, P., Hekman, R.M., Tamura, T., et al., 2022. Humanized mice reveal a macrophage-enriched gene signature defining human lung tissue protection during SARS-CoV-2 infection. *Epub 20220404 Cell Rep.* 39 (3), 110714. <https://doi.org/10.1016/j.celrep.2022.110714>. PubMed PMID: 35421379; PubMed Central PMCID: PMCPCMC8977517.
- Khan, M.A., Khan, A., 2021. Role of NKT cells during viral infection and the development of NKT cell-based nanovaccines. *Vaccines* 9 (9), 949. <https://doi.org/10.3390/vaccines9090949>.
- Khan, M., Yoo, S.J., Clijsters, M., Backaert, W., Vanstapel, A., Speleman, K., et al., 2021. Visualizing in deceased COVID-19 patients how SARS-CoV-2 attacks the respiratory and olfactory mucosae but spares the olfactory bulb. *e15*. *Epub 20211103 Cell* 184 (24), 5932–5949. <https://doi.org/10.1016/j.cell.2021.10.027>. PubMed PMID: 34798069; PubMed Central PMCID: PMCPCMC8564600.

- Khan, M., Clijsters, M., Choi, S., Backaert, W., Claeherout, M., Couvreur, F., et al., 2022. Anatomical barriers against SARS-CoV-2 neuroinvasion at vulnerable interfaces visualized in deceased COVID-19 patients. *Epub 20221110 Neuron*. <https://doi.org/10.1016/j.neuron.2022.11.007>. PubMed PMID: 36446381.
- Kreutmaier, S., Unger, S., Nunez, N.G., Ingelfinger, F., Alberti, C., De Feo, D., et al., 2021. Distinct immunological signatures discriminate severe COVID-19 from non-SARS-CoV-2-driven critical pneumonia. *e5*. *Epub 2021/05/30 Immunity* 54 (7), 1578–1593. <https://doi.org/10.1016/j.immuni.2021.05.002>. PubMed PMID: 34051147; PubMed Central PMCID: PMCPCMC8106882.
- Kumari, P., Rothan, H.A., Natekar, J.P., Stone, S., Pathak, H., Strate, P.G., et al., 2021. Neuroinvasion and encephalitis following intranasal inoculation of SARS-CoV-2 in K18-hACE2 mice. *Epub 20210119 Viruses* 13 (1). <https://doi.org/10.3390/v13010132>. PubMed PMID: 33477869; PubMed Central PMCID: PMCPCMC7832889.
- Lapuenta, D., Fuchs, J., Willar, J., Vieira Antão, A., Eberlein, V., Uhlig, N., et al., 2021. Protective mucosal immunity against SARS-CoV-2 after heterologous systemic prime-mucosal boost immunization. *Epub 2021/11/28 Nat. Commun.* 12 (1), 6871. <https://doi.org/10.1038/s41467-021-27063-4>. PubMed PMID: 34836955; PubMed Central PMCID: PMCPCMC8626513 no competing interests.
- Leist, S.R., Dinnon 3rd, K.H., Schäfer, A., Tse, L.V., Okuda, K., Hou, Y.J., et al., 2020. A mouse-adapted SARS-CoV-2 induces acute lung injury and mortality in standard laboratory mice. *e12*. *Epub 2020/10/09 Cell* 183 (4), 1070–1085. <https://doi.org/10.1016/j.cell.2020.09.050>. PubMed PMID: 33031744; PubMed Central PMCID: PMCPCMC7510428.
- Li, J., Jia, H., Tian, M., Wu, N., Yang, X., Qi, J., et al., 2022. SARS-CoV-2 and emerging variants: unmasking structure, function, infection, and immune escape mechanisms. *Epub 20220512 Front. Cell. Infect. Microbiol.* 12, 869832. <https://doi.org/10.3389/fcimb.2022.869832>. PubMed PMID: 35646741; PubMed Central PMCID: PMCPCMC9134119.
- Mao, T., Israelow, B., Lucas, C., Vogels, C.B.F., Gomez-Calvo, M.L., Fedorova, O., et al., 2021. A stem-loop RNA RIG-I agonist protects against acute and chronic SARS-CoV-2 infection in mice. *J. Exp. Med.* 219 (1), e20211818 <https://doi.org/10.1084/jem.20211818>.
- Mao, T., Israelow, B., Suberi, A., Zhou, L., Reschke, M., Peña-Hernández, M.A., et al., 2022. Unadjuvanted intranasal spike vaccine elicits robust protective mucosal immunity against sarbecoviruses. *Epub 2022/02/05 bioRxiv*. <https://doi.org/10.1101/2022.01.24.477597>. PubMed PMID: 35118464; PubMed Central PMCID: PMCPCMC8811895.
- Mazzoni, A., Salvati, L., Maggi, L., Capone, M., Vanni, A., Spinicci, M., et al., 2020. Impaired immune cell cytotoxicity in severe COVID-19 is IL-6 dependent. *Epub 2020/05/29 J. Clin. Invest.* 130 (9), 4694–4703. <https://doi.org/10.1172/JCI138554>. PubMed PMID: 32463803; PubMed Central PMCID: PMCPCMC7456250.
- McCray Jr., P.B., Pewe, L., Wohlford-Lenane, C., Hickey, M., Manzel, L., Shi, L., et al., 2020. Lethal infection of K18-hACE2 mice infected with severe acute respiratory syndrome coronavirus. *Epub 2006/11/03 J. Virol.* 81 (2), 813–821. <https://doi.org/10.1128/JVI.02012-06>. PubMed PMID: 17079315; PubMed Central PMCID: PMCPCMC1797474.
- Meinhardt, J., Radke, J., Dittmayer, C., Franz, J., Thomas, C., Mothes, R., et al., 2021. Olfactory transmucosal SARS-CoV-2 invasion as a port of central nervous system entry in individuals with COVID-19. *Epub 20211130 Nat. Neurosci.* 24 (2), 168–175. <https://doi.org/10.1038/s41593-020-00758-5>. PubMed PMID: 33257876.
- Mohandas, S., Yadav, P.D., Sapkal, G., Shete, A.M., Deshpande, G., Nyayanit, D.A., et al., 2022. Pathogenicity of SARS-CoV-2 Omicron (R346K) variant in Syrian hamsters and its cross-neutralization with different variants of concern. *Epub 20220408 EBioMedicine* 79, 103997. <https://doi.org/10.1016/j.ebiom.2022.103997>. PubMed PMID: 35405385; PubMed Central PMCID: PMCPCMC8993158.
- Montagutelli, X., Prot, M., Levillayer, L., Salazar, E.B., Jouvion, G., Conquet, L., et al., 2021. The B1.351 and P.1 variants extend SARS-CoV-2 host range to mice. *Epub 2021/03/18.436013 bioRxiv*. <https://doi.org/10.1101/2021.03.18.436013>.
- Natekar, J.P., Pathak, H., Stone, S., Kumari, P., Sharma, S., Auroon, T.T., et al., 2022. Differential pathogenesis of SARS-CoV-2 variants of concern in human ACE2-expressing mice. *Epub 20220525 Viruses* 14 (6). <https://doi.org/10.3390/v14061139>. PubMed PMID: 35746611; PubMed Central PMCID: PMCPCMC9231291.
- Perry, V.H., Cunningham, C., Holmes, C., 2007. Systemic infections and inflammation affect chronic neurodegeneration. *Epub 20070115 Nat. Rev. Immunol.* 7 (2), 161–167. <https://doi.org/10.1038/nri2015>. PubMed PMID: 17220915.
- Rathnasinghe, R., Jangra, S., Cupic, A., Martínez-Romero, C., Mulder, L.C.F., Kehrer, T., et al., 2021. The N501Y mutation in SARS-CoV-2 spike leads to morbidity in obese and aged mice and is neutralized by convalescent and post-vaccination human sera. *Epub 2021/01/28 medRxiv*. <https://doi.org/10.1101/2021.01.19.21249592>. PubMed PMID: 33501468; PubMed Central PMCID: PMCPCMC7836140 Pfizer, Senhwa Biosciences, Kenall Manufacturing, Avimex, Johnson & Johnson, Dynavax, 7Hills Pharma, ImmunityBio and Nanocomposix. Dr. Adolfo García-Sastre has consulting agreements for the following companies involving cash and/or stock: Vivaldi Biosciences, Contrafect, 7Hills Pharma, Avimex, Vaxalto, Pagoda, Accurix and Esperovax. Mount Sinai has licensed SARS-CoV-2 serological assays to commercial entities and has filed for patent protection for serological assays as well as SARS-CoV-2 vaccines. F.K. is listed as inventors on the pending patent applications. The F.K. laboratory has received research support from GSK, Dynavax and Pfizer. F.K. has in the past received consulting fees from Curevac, Merck, Pfizer and Seqirus. A provisional patent application on a “A novel 4 Amino Acid Insertion into the Spike Protein of SARS-CoV-2” was submitted by KSU in July 2020 with C.D. M., D.A.M and J.A.R listed as inventors.
- Rhea, E.M., Logsdon, A.F., Hansen, K.M., Williams, L.M., Reed, M.J., Baumann, K.K., et al., 2021. The S1 protein of SARS-CoV-2 crosses the blood-brain barrier in mice. *Epub 20201216 Nat. Neurosci.* 24 (3), 368–378. <https://doi.org/10.1038/s41593-020-00771-8>. PubMed PMID: 33328624; PubMed Central PMCID: PMCPCMC8793077.
- Rutkai, I., Mayer, M.G., Hellmers, L.M., Ning, B., Huang, Z., Monjure, C.J., et al., 2022. Neuropathology and virus in brain of SARS-CoV-2 infected non-human primates. *Epub 20220401 Nat. Commun.* 13 (1), 1745. <https://doi.org/10.1038/s41467-022-29440-z>. PubMed PMID: 35365631; PubMed Central PMCID: PMCPCMC8975902.
- Rydzynski Moderbacher, C., Ramirez, S.L., Dan, J.M., Grifoni, A., Hastie, K.M., Weiskopf, D., et al., 2020. Antigen-specific adaptive immunity to SARS-CoV-2 in acute COVID-19 and associations with age and disease severity. *e19*. *Epub 2020/10/05 Cell* 183 (4), 996–1012. <https://doi.org/10.1016/j.cell.2020.09.038>. PubMed PMID: 33010815; PubMed Central PMCID: PMCPCMC7494270.
- Satturwar, S., Fowkes, M., Farver, C., Wilson, A.M., Eecher, A., Girolami, I., et al., 2021. Postmortem findings associated with SARS-CoV-2: systematic review and meta-analysis. *Am. J. Surg. Pathol.* 45 (5), 587–603. <https://doi.org/10.1097/pas.0000000000001650>. PubMed PMID: 33481385; PubMed Central PMCID: PMCPCMC8132567.
- Seehusen, F., Clark, J.J., Sharma, P., Bentley, E.G., Kirby, A., Subramaniam, K., et al., 2022. Neuroinvasion and neurotropism by SARS-CoV-2 variants in the K18-hACE2 mouse. *Epub 20220511 Viruses* 14 (5). <https://doi.org/10.3390/v14051020>. PubMed PMID: 35632761; PubMed Central PMCID: PMCPCMC9146514.
- Sefik, E., Israelow, B., Zhao, J., Qu, R., Song, E., Mirza, H., et al., 2021. A humanized mouse model of chronic COVID-19 to evaluate disease mechanisms and treatment options. *Epub 2021/03/25 Res Sq*. <https://doi.org/10.21203/rs.3.rs-279341/v1>. PubMed PMID: 33758831; PubMed Central PMCID: PMCPCMC7987100.
- Sefik, E., Qu, R., Junqueira, C., Kaffe, E., Mirza, H., Zhao, J., et al., 2022. Inflammation activation in infected macrophages drives COVID-19 pathology. *Epub 20220428 Nature*. <https://doi.org/10.1038/s41586-022-04802-1>. PubMed PMID: 35483404.
- Sekine, T., Perez-Potti, A., Rivera-Ballesteros, O., Strálin, K., Gorin, J.-B., Olsson, A., et al., 2020. Robust T cell immunity in convalescent individuals with asymptomatic or mild COVID-19. *Cell* 183 (1), 158–168. <https://doi.org/10.1016/j.cell.2020.08.017>.
- Serrano, G.E., Walker, J.E., Tremblay, C., Piras, I.S., Huentelman, M.J., Belden, C.M., et al., 2022. SARS-CoV-2 brain regional detection, histopathology, gene expression, and immunomodulatory changes in decedents with COVID-19. *J. Neuroopathol. Exp. Neurol.* 81 (9), 666–695. <https://doi.org/10.1093/jnen/nlnc056>. PubMed PMID: 35818336; PubMed Central PMCID: PMCPCMC9278252.
- Shang, C., Zhuang, X., Zhang, H., Li, Y., Zhu, Y., Lu, J., et al., 2021. Inhibition of autophagy suppresses SARS-CoV-2 replication and ameliorates pneumonia in hACE2 transgenic mice and xenografted human lung tissues. *Epub 20210922 J. Virol.* 95 (24), e0153721. <https://doi.org/10.1128/jvi.01537-21>. PubMed PMID: 34550769; PubMed Central PMCID: PMCPCMC8610582.
- Shang, W., Dai, W., Yao, C., Xu, L., Tao, X., Su, H., et al., 2022. In vitro and in vivo evaluation of the main protease inhibitor FB2001 against SARS-CoV-2. *Epub 20221029 Antivir. Res.* 208, 105450. <https://doi.org/10.1016/j.antiviral.2022.105450>. PubMed PMID: 36354082; PubMed Central PMCID: PMCPCMC9617675.
- Shultz, L.D., Ishikawa, F., Greiner, D.L., 2007. Humanized mice in translational biomedical research. *Nat. Rev. Immunol.* 7 (2), 118–130. <https://doi.org/10.1038/nri2017>.
- Song, E., Zhang, C., Israelow, B., Lu-Culligan, A., Prado, A.V., Skriabine, S., et al., 2021. Neuroinvasion of SARS-CoV-2 in human and mouse brain. *J. Exp. Med.* 218 (3) <https://doi.org/10.1084/jem.20202135>. PubMed PMID: 33433624; PubMed Central PMCID: PMCPCMC7808299.
- Starr, T.N., Greaney, A.J., Stewart, C.M., Walls, A.C., Hannon, W.W., Veessler, D., et al., 2022. Deep mutational scans for ACE2 binding, RBD expression, and antibody escape in the SARS-CoV-2 Omicron BA.1 and BA.2 receptor-binding domains. *Epub 20221118 PLoS Pathog.* 18 (11), e1010951. <https://doi.org/10.1371/journal.ppat.1010951>. PubMed PMID: 36399443; PubMed Central PMCID: PMCPCMC9674177.
- Swadlow, L., Diniz, M.O., Schmidt, N.M., Amin, O.E., Chandran, A., Shaw, E., et al., 2022. Pre-existing polyclonal T cells expand in abortive seronegative SARS-CoV-2. *Nature* 601 (7891), 110–117. <https://doi.org/10.1038/s41586-021-04186-8>.
- Tan, L., Wang, Q., Ding, J., Huang, Q., Tang, Y.Q., et al., 2020. Lymphopenia predicts disease severity of COVID-19: a descriptive and predictive study. *Epub 2020/04/17 Signal Transduct. Targeted Ther.* 5 (1), 33. <https://doi.org/10.1038/s41392-020-0148-4>. PubMed PMID: 32296069; PubMed Central PMCID: PMCPCMC7100419.
- Taquet, M., Sillett, R., Zhu, L., Mendel, J., Camplisson, I., Dercon, Q., et al., 2022. Neurological and psychiatric risk trajectories after SARS-CoV-2 infection: an analysis of 2-year retrospective cohort studies including 1 284 437 patients. *Epub 20220817 Lancet Psychiatr.* 9 (10), 815–827. [https://doi.org/10.1016/s2215-0366\(22\)00260-7](https://doi.org/10.1016/s2215-0366(22)00260-7). PubMed PMID: 35987197; PubMed Central PMCID: PMCPCMC9385200.
- Tarke, A., Sidney, J., Kidd, C.K., Dan, J.M., Ramirez, S.I., Yu, E.D., et al., 2021. Comprehensive analysis of T cell immunodominance and immunoprevalence of SARS-CoV-2 epitopes in COVID-19 cases. *Epub 2021/02/02 Cell Rep. Med.* 2 (2), 100204. <https://doi.org/10.1016/j.xcrm.2021.100204>. PubMed PMID: 33521695; PubMed Central PMCID: PMCPCMC7837622.
- Tarpinian, S., Rowe, J., Husanov, R., Saha, U., Banerjee, P., Eraslan, R., et al., 2020. 247 Assessment of sensitivity to a PD-1 check point inhibitor and cisplatin in bladder cancer patient-derived xenografts with various levels of PD-L1 expression in HuCD34NCG mice. *J. Immunother. Cancer* 8 (Suppl. 3). <https://doi.org/10.1136/jitc-2020-SITC2020.0247>. A147-A.
- Vidal, E., López-Figueroa, C., Rodon, J., Pérez, M., Brustolin, M., Cantero, G., et al., 2021. Chronological brain lesions after SARS-CoV-2 infection in hACE2-transgenic mice. *Vet. Pathol.* 59 (4), 613–626. <https://doi.org/10.1177/03009858211066841>.

- Wahl, A., Gralinski, L.E., Johnson, C.E., Yao, W., Kovarova, M., Dinnon 3rd, K.H., et al., 2021. SARS-CoV-2 infection is effectively treated and prevented by EIDD-2801. *Epub 20210209 Nature* 591 (7850), 451–457. <https://doi.org/10.1038/s41586-021-03312-w>. PubMed PMID: 33561864; PubMed Central PMCID: PMCPCMC7979515.
- Wang, Y.T., Landeras-Bueno, S., Hsieh, L.E., Terada, Y., Kim, K., Ley, K., et al., 2020a. Spiking pandemic potential: structural and immunological aspects of SARS-CoV-2. *Epub 2020/06/09 Trends Microbiol.* 28 (8), 605–618. <https://doi.org/10.1016/j.tim.2020.05.012>. PubMed PMID: 32507543; PubMed Central PMCID: PMCPCMC7237910.
- Wang, D., Hu, B., Hu, C., Zhu, F., Liu, X., Zhang, J., et al., 2020b. Clinical characteristics of 138 hospitalized patients with 2019 novel coronavirus-infected pneumonia in Wuhan, China. *Epub 2020/02/08 JAMA* 323 (11), 1061–1069. <https://doi.org/10.1001/jama.2020.1585>. PubMed PMID: 32031570; PubMed Central PMCID: PMCPCMC7042881.
- Wang, J., Zheng, X., Chen, J., 2021. Clinical progression and outcomes of 260 patients with severe COVID-19: an observational study. *Sci. Rep.* 11 (1), 3166. <https://doi.org/10.1038/s41598-021-82943-5>.
- Wang, L., Davis, P.B., Volkow, N.D., Berger, N.A., Kaelber, D.C., Xu, R., 2022. Association of COVID-19 with new-onset Alzheimer's disease. *J. Alzheimer. Dis.* 89, 411–414. <https://doi.org/10.3233/JAD-220717>.
- WHO, 2023. Tracking SARS-CoV-2 variants [cited 2023]. Available from: <https://www.who.int/activities/tracking-SARS-CoV-2-variants>.
- Winkler, E.S., Chen, R.E., Alam, F., Yildiz, S., Case, J.B., Uccellini, M.B., et al., 2022. SARS-CoV-2 causes lung infection without severe disease in human ACE2 knock-in mice. *Epub 2021/10/21 J. Virol.* 96 (1), e0151121. <https://doi.org/10.1128/JVI.01511-21>. PubMed PMID: 34668780; PubMed Central PMCID: PMCPCMC8754206.
- Yang, X., Yu, Y., Xu, J., Shu, H., Xia, J., Liu, H., et al., 2020. Clinical course and outcomes of critically ill patients with SARS-CoV-2 pneumonia in Wuhan, China: a single-centered, retrospective, observational study. *Epub 2020/02/28 Lancet Respir. Med.* 8 (5), 475–481. [https://doi.org/10.1016/s2213-2600\(20\)30079-5](https://doi.org/10.1016/s2213-2600(20)30079-5). PubMed PMID: 32105632; PubMed Central PMCID: PMCPCMC7102538.
- Zhang, L., Zhou, L., Bao, L., Liu, J., Zhu, H., Lv, Q., et al., 2021. SARS-CoV-2 crosses the blood-brain barrier accompanied with basement membrane disruption without tight junctions alteration. *Epub 20210906 Signal Transduct. Targeted Ther.* 6 (1), 337. <https://doi.org/10.1038/s41392-021-00719-9>. PubMed PMID: 34489403; PubMed Central PMCID: PMCPCMC8419672.
- Zhang, P.-P., He, Z.-C., Yao, X.-H., Tang, R., Ma, J., Luo, T., et al., 2023. COVID-19-associated monocytic encephalitis (CAME): histological and proteomic evidence from autopsy. *Signal Transduct. Targeted Ther.* 8 (1), 24. <https://doi.org/10.1038/s41392-022-01291-6>.
- Zheng, J., Wong, L.R., Li, K., Verma, A.K., Ortiz, M.E., Wohlford-Lenane, C., et al., 2021. COVID-19 treatments and pathogenesis including anosmia in K18-hACE2 mice. *Epub 20201109 Nature* 589 (7843), 603–607. <https://doi.org/10.1038/s41586-020-2943-z>. PubMed PMID: 33166988; PubMed Central PMCID: PMCPCMC7855185.
- Zhou, F., Yu, T., Du, R., Fan, G., Liu, Y., Liu, Z., et al., 2020. Clinical course and risk factors for mortality of adult inpatients with COVID-19 in Wuhan, China: a retrospective cohort study. *Epub 2020/03/15 Lancet* 395 (10229), 1054–1062. [https://doi.org/10.1016/s0140-6736\(20\)30566-3](https://doi.org/10.1016/s0140-6736(20)30566-3). PubMed PMID: 32171076; PubMed Central PMCID: PMCPCMC7270627.
- Zhu, N., Zhang, D., Wang, W., Li, X., Yang, B., Song, J., et al., 2020. A novel coronavirus from patients with pneumonia in China, 2019. *Epub 20200124 N. Engl. J. Med.* 382 (8), 727–733. <https://doi.org/10.1056/NEJMoa2001017>. PubMed PMID: 31978945; PubMed Central PMCID: PMCPCMC7092803.
- Zingaropoli, M.A., Perri, V., Pasculli, P., Cogliati Dezza, F., Nijhawan, P., Savelloni, G., et al., 2021. Major reduction of NKT cells in patients with severe COVID-19 pneumonia. *Epub 2020/11/16 Clin. Immunol.* 222, 108630. <https://doi.org/10.1016/j.clim.2020.108630>. PubMed PMID: 33189887; PubMed Central PMCID: PMCPCMC7661928.